

E.S. Battistelli¹, M. Amiri¹, B. Burger¹, M.
Halpern¹, S. Knotek¹, M. Ellis², X. Gao²,
D. Kelly², M. MacIntosh², K. Irwin³, C.
Reintsema³

Functional description of read-out electronics for time-domain multiplexed bolometers for millimeter and sub-millimeter astronomy

22.07.2007

Keywords Read-out electronics, SQUID, time-domain multiplexing, millimeter and sub-millimeter astronomy

Abstract We have developed multi-channel electronics (MCE) which work in concert with time-domain multiplexors developed at NIST, to control and read signals from large format bolometer arrays of superconducting transition edge sensors (TESs). These electronics were developed as part of the Submillimeter Common-User Bolometer Array 2 (SCUBA2) camera, but are now used in several other instruments. The main advantages of these electronics compared to earlier versions is that they are multi-channel, fully programmable, suited for remote operations and provide a clean geometry, with no electrical cabling outside of the Faraday cage formed by the cryostat and the electronics chassis.

The MCE is used to determine the optimal operating points for the TES and the superconducting quantum interference device (SQUID) amplifiers autonomously. During observation, the MCE execute a running PID-servo and applies to each first stage SQUID a *feedback* signal necessary to keep the system in a linear regime at optimal gain. The feedback and error signals from a ~ 1000 -pixel array can be written to hard drive at up to 2kHz.

PACS numbers: 95.55.Rg; 95.55.Sh; 95.85.Bh; 95.85.fm; 98.80.Es

1 Introduction

Millimeter (mm) and sub-millimeter (sub-mm) astronomy is undergoing a revolution thanks to the development of new cameras based on bolometer arrays of

1: Department of Physics and Astronomy, University of British Columbia
6224 Agricultural Road Vancouver, B.C. Canada, V6T 1Z1

Tel.: +1 604 822 6709; Fax: +1 604 822 1938; E-mail: elia@phas.ubc.ca

2: UK Astronomy Technology Centre, ROE, Edinburgh, Scotland

3: National Institute of Standards and Technology (NIST), Boulder, Colorado.

TESs. These cameras will provide the sensitivity and mapping speed needed to perform high precision cosmic microwave background (CMB) measurements and accurate characterization of extragalactic sub-mm galaxies. TES arrays are coupled to SQUIDs that ensure high bandwidth and low noise signal read-out.

Once detectors are photon noise limited, an increase in the number of pixels is needed to improve the sensitivity. Massive increase of the number of pixels in a mm and sub-mm camera is now possible thanks to the development of multiplexing techniques that reduce the number of wires reaching the cold stages of the cryostat housing the detectors. The MCE described here use 50 times fewer wires per pixel than low noise electronics designed for single pixel Neutron Transmutation Doped bolometers¹.

Highly specialized electronics are needed for these systems and a continuous research activity is required to suite and tailor the electronics for the specific needs of an instrument. At U.B.C. we have developed ambient temperature multi-channel electronics (MCE) which work in concert with time-domain multiplexors developed at NIST, Boulder² for large format arrays of TES bolometers. The system borrows from an early design developed by NIST³. The MCE were initially developed for SCUBA2⁴ and are used as read-out electronics on many CMB and sub-mm astronomy experiments (*e.g.* ACT⁵, CℓOVER⁶, Spider⁷, BICEPII⁸, and SPUD⁸).

In section 2 we give a general description of the MCE, in section 3 we present the functional blocks which form the MCE and in section 4 we give some highlights of the capabilities and *modus operandi* of the MCE.

2 MCE general description

The MCE set the detector bias, control the multiplexor and three-stage, SQUID-based amplifiers and read the signals from an array of up to 32×41 pixels. Cameras often have several arrays in a single cryostat in order to operate at several wavelengths (*e.g.* ACT) or to fill a larger focal plane (*e.g.* SCUBA2). Each array is connected via hermetic cryogenic cables to a single box of MCE which is mounted to the cryostat wall. The MCE are in turn connected by an optical fibre to a data-acquisition computer. All commands and data run through this fibre. Thus the *only* necessary electrical connection to the cryostat and electronics is a single DC voltage for power.

The data acquisition computer sends commands to the MCE and receives data packets. Data Acquisition Software (DAS), developed at the Astronomy Technology Center, Edinburgh, is based on a system running RTAI Linux. Data are packaged by the MCE into frames containing a housekeeping block followed by a data block and a checksum. The data block is (32×41) 32-bit numbers and nominally contains one value from each pixel. The MCE can be commanded to return one frame of data, to return N numbered frames timed using an internal crystal clock, or to return N numbered frames taking the timing from an external synch pulse. The MCE can support frame rates of several kHz, but in most cameras 200 Hz is sufficient.

A triggerable Synchronization Box supplies numbered Data Valid Pulses (DVP) bi-phase encoded into a 25 MHz clock to all MCE boxes via optical fibre. The Syn-

chronization Box has extra outputs, allowing these numbered pulses to be used to synchronize collection of telescope pointing system and housekeeping data.

In the standard data mode, the MCE report low-pass filtered feedback values for each pixel. An alternate mode reports error and feedback signals mixed into each 32-bit word. Engineering modes are available which report signals at up to 20kHz or even bursts of 50-MHz data.

There is an Altera¹ Field Programmable Gate Array (FPGA) on each of the MCE cards with the exception of the power supply card. These provide the flexibility of field upgrades. More importantly, they offer the option of running the electronics in several different modes and of tailoring them to different array geometries. The firmware has been developed in VHDL and comprises a fair fraction of the total effort of developing the MCE.

In a MCE subrack, a Bus Backplane (BB) and an Instrument Backplane (IB) enable card-to-card communication, power distribution and connection to cryostat analog signals. Custom capacitive filter circuits are built on the MCE-cryostat interface and represent the input/output gates to the Faraday cage enclosure of the cryostat and the MCE's connector enclosures.

The power for the MCE is supplied through a pluggable switching-mode Power Supply Card (PSC) that is powered from an external AC-to-DC Unit (ACDCU). This solution allows for flexible grounding and noise isolation as well as the ability to remotely power cycle the MCE.

3 MCE functional block descriptions

3.1 SQUID Bias Control

The voltage across a SQUID varies periodically with the magnetic flux through it, and the amplitude of this $V \cdot \phi$ variation depends on a bias current through the SQUID. In the NIST multiplexors and amplifiers, each SQUID has two flux inputs: one is a signal input and the other, which we call *feedback*, can be used to compensate the input level and hold the SQUID near the point of highest slope in the $V \cdot \phi$ curve. Setting up an array consists of choosing a bias current and a feedback flux input for every SQUID.

The first-stage SQUIDs (SQ1s) coupled to each pixel are controlled by the multiplexing and signal reading cards whose functionality is described in the following sections. The bias currents for the second stage SQUIDs (SQ2) and the high gain SQUID series array modules (SSAM) vary slowly and are controlled by up to three commandable Bias Cards (BCs), each of which has 32 16-bit DACs with high-stability and low-noise. Warm low noise load resistors on the IB set the current corresponding to full scale for each bias channel.

In addition to these SQUID biases, ultra low noise differential outputs provide a commandable bias voltage for the TES bolometers and an optional pixel heater. These are lowpass-filtered to 10kHz and fed to low-noise, high-stability (± 10 ppm/ $^{\circ}$ C) load resistors. For SCUBA2 the MCE generate one TES bias and one Pixel Heater current, but for other cameras up to 16 independently commanded TES bias values are supplied.

¹ <http://www.altera.com/>

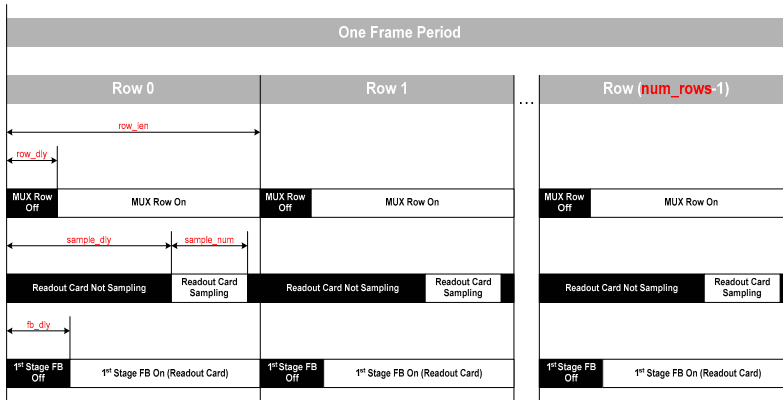


Fig. 1 MCE frame timing structure. All the quantities can be specified in 50-MHz cycles. On the top the AC firmware *row_dly* setting and on the bottom the RC timing parameters for signal reading, (*sample_dly* and *sample_num*) and for supplying the SQ1 *feedback* (*fb_dly*).

3.2 Multiplexing Control

In a typical time-domain multiplexing configuration the SQ1 signals of one *column* of an array are summed in a coil coupled to one SQ2 and consequently amplified by one channel of a SSAM. Multiplexing an array consists of turning on one *row* of SQ1s at a time. This task is performed by the MCE’s Address Card (AC) which drives each row using a 14-bit video DAC with 0-1V voltage range.

The AC’s firmware controls up to 41 DACs through a block that has the following features: (1) the row order is user-specifiable; (2) the multiplexing can be enabled or disabled by command; (3) the delay between the start of a row-dwell period and the assertion of the *on* value on the DAC can be specified in terms of 50-MHz clock cycles; (4) the AC supports separate *on* and *off* values for each row. For any given row the optimal *on* bias value is a compromise between the SQ1s across the 32 columns.

The typical dwell time per row is near to $1\mu\text{s}$. In a 41 row array, this dwell time results in re-visiting the whole array at a frequency of $\sim 20\text{ kHz}$.

3.3 Pixel Read-out

A voltage biased TES bolometer element will operate at its superconducting transition temperature. The current flowing through it is reduced if the optical power incident upon it increases. Exploiting the intrinsic non-linearity of the SQUID’s response, a digital Proportional Integral Differential feedback servo loop (PID loop) is used to calculate the correct flux to be sent to the SQ1 *feedback* to compensate for changes in detector current and to keep the amplification chain in a linear regime. These feedback values constitute a measurement of the optical input power and are the nominal *outputs* of the MCE.

Readout Cards (RC) are coupled to eight columns and handle PID loops for 8×41 pixels independently. In synchronization with the multiplexer, the PID output based on the reading from the previous visit to a given row is applied to the

SQ1 *feedback* using 14-bit video DAC with 0-1V voltage range. Each column output from the SSAM is fed to a preamplifier followed by a 14-bit, 50-MHz video ADC. After allowing for settling, *SAMPLE_NUM* readings are summed to form an error signal, which acts as the next input to the PID loop.

The pixel-visit frequency of 20 kHz far exceeds the detector bandwidth set by the thermal response time. In order to reduce in-band aliasing, a 4-pole Butterworth IIR low pass filter with a cut off consistent with the detector thermal time constant is implemented.

The RCs provide the highest electrical and firmware design challenge in the MCE, and they consume the most power.

3.4 Communication

Communications between the MCE and the data acquisition PC are through a duplex fibre optic cable. The MCE's inter-card communications are via busses LVDS links. The MCE's Clock Card (CC) receives DAS commands, dispatches commands to cards, receives card replies, assembles replies into packets, and sends the packets back to the DAS PC. In addition, the CC autonomously issues internal commands to monitor the status of the MCE, and returns the data collected in packet headers. The CC also has a fibre interface for the Synchronization Box's DVP, and a JTAG interface for programming the MCE's devices.

The CC generates a 25-MHz clock derived from either an on-board crystal or an external source which is then distributed to the other cards in the MCE. Upon receipt of a data request command, the CC waits for completion of one multiplexing cycle, and then: (1) requests the data package from each RC; (2) requests other housekeeping data from all cards; (3) assembles a frame of data; (4) sends the data frame to the data acquisition computer.

4 Using the MCE to characterize an array of detectors

During array setup the SQUIDs typically have to be biased at the critical current I_C^{max} and the feedback currents chosen to maximize linearity and gain on the $V \cdot \phi$ curve. Our automatic software-developed array characterization starts from the SSAM, proceeds to the SQ2 stage and then to the SQ1 stage.

For the SSAM stage, a simple 2-dimensional grid of output voltage vs feedback voltage is collected for different SSAM bias currents, and the bias which produces the maximum peak to peak modulation for each $V \cdot \phi$ curve (*i.e.* I_C^{max}) is selected. For the chosen bias current, the SSAM output voltage corresponding to the maximum slope of the $V \cdot \phi$ curve is selected as the set-point in the next stage of the set-up. The same method cannot be directly applied to the SQ2s since the resulting curve would not be a simple combination of the two $V \cdot \phi$ curves. Thus, we measure the SQ2 $V \cdot \phi$ curves using a closed servo loop. For a given value of the SQ2 bias current, we sweep the SQ2 feedback current from zero to full scale. At each value of the SQ2 feedback current, software adjusts the SSAM feedback current to bring the SSAM output back to the target output voltage chosen above. The resulting curves (*i.e.* SSAM *feedback* vs SQ2 *feedback*) are now representative of the SQ2 $V \cdot \phi$ curves allowing choice of SQ2 bias and SSAM *feedback* values

corresponding to optimal gain. An identical technique is used for the SQ1 stage allowing to choose SQ1 bias and SQ2 feedback currents. In this case, however, the SQ1 bias currents are chosen as a compromise among the 32 SQ1s of each row and each SQ2 *feedback* value is again a compromise among the 41 SQ1s in a given column. The final step of the locking procedure is an open loop acquisition of the SSAM output of each pixel of the array while sweeping the SQ1 *feedback*. This allows a fine tuning of the DC offsets, this time chosen on a pixel basis.

Once array optimization is complete, the servo PID loop can be switched on and the full array comes into lock. The P , I and D gains can be commanded independently for each pixel. Array characterization typically takes place with the array locked. For example, TES $I - V$ curves are collected for all pixels at once by alternately commanding a new TES bias current and collecting a single frame of unfiltered data. The full automated process takes two minutes.

We have explored variations on the above procedures made possible by the programmability of the electronics: a) if an AC is used in place of one of the SQ2 BCs, the SQ2 feedback can be switched at the Row Select rate. In this mode, the SQ2 feedback value is no longer a compromise among the 41 rows; b) the SQ1 *feedback* signal can be a ramp equal to N flux constants. The output of the amplifier becomes a periodic wave, and the optical signal corresponds to the phase of that wave. This mode eliminates some magnetic pickup terms; c) if an array is used with a polarimeter, the IIR filter implemented in the RCs can be replaced with digital lock-in amplifiers so that I , Q and U are direct outputs of the MCE.

5 Conclusions

At the University of British Columbia we develop ambient-temperature Multi-channel Electronics for interfacing with large-format bolometric arrays of TES. The functionality of the MCE is verified during extensive component-level, module-level and system-level tests. The measured low noise and stability of the MCE mean that the overall system noise is limited by the TES and SQUID circuits.

Acknowledgements We thank Dan Bintley, Norm Jarosik, Jan Kycia, Mike Neimack, Suzanne Staggs and especially Tom Felton. The MCE project is funded by the Canadian Foundation for Innovation and managed by Janos Molnar. ESB wishes to thank the National Science and Engineering Research Council (NSERC).

References

1. H. P. Gush *et al.* *Review of scientific Instruments*, **63**,90,(1992)
2. P. A. de Korte *et al.*, *Rev. of Sci. Inst.* **74**, 8, 3807-15, (2003).
3. C. D. Reintsema *et al.*, *Rev. of Sci. Inst.*,**74**, 10, 4500 (2003).
4. W. S. Holland *et al.* *Proceedings of the SPIE*, **6275**, 62751E (2006).
5. J. Fowler *et al.* *App. Optics* **45**, 3746, (2006).
6. M. D. Audley *et al.* *Proceedings of the SPIE*, **6275**, 627524 (2006).
7. T. E. Montroy *et al.* *Proceedings of the SPIE*, **6267**, 62670R (2006)
8. J. Kovac *et al.* *Bulletin of the American Astronomical Society*, **38**, 913 (2006)
9. J.A. Bailey *et al.* *Proceedings of the SPIE*, **2479**, 62-68 (1995)